



Universiteit  
Leiden  
The Netherlands

## Pyroptosis-inducing active caspase-1 as a genetic adjuvant in anti-cancer DNA vaccination

Arakelian, T.; Oosterhuis, K.; Tondini, E.; , M. los; Vree, J.; Geldorp, M. van; ... ; Bergen, J. van

### Citation

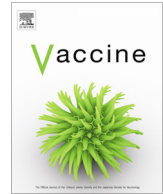
Arakelian, T., Oosterhuis, K., Tondini, E., Vree, J., Geldorp, M. van, Camps, M., ... Bergen, J. van. (2022). Pyroptosis-inducing active caspase-1 as a genetic adjuvant in anti-cancer DNA vaccination. *Vaccine*, 40(13), 2087-2098. doi:10.1016/j.vaccine.2022.02.028

Version: Publisher's Version

License: [Creative Commons CC BY 4.0 license](https://creativecommons.org/licenses/by/4.0/)

Downloaded from: <https://hdl.handle.net/1887/3486985>

**Note:** To cite this publication please use the final published version (if applicable).



## Pyroptosis-inducing active caspase-1 as a genetic adjuvant in anti-cancer DNA vaccination



Tsolere Arakelian<sup>a</sup>, Koen Oosterhuis<sup>b,a,1</sup>, Elena Tondini<sup>a,1</sup>, Mandy Los<sup>b</sup>, Jana Vree<sup>a</sup>, Mariska van Geldorp<sup>a</sup>, Marcel Camps<sup>a</sup>, Bram Teunisse<sup>b</sup>, Iris Zoutendijk<sup>c</sup>, Ramon Arens<sup>a</sup>, Gerben Zondag<sup>b,c</sup>, Ferry Ossendorp<sup>a,2,\*</sup>, Jeroen van Bergen<sup>b,a,2,\*</sup>

<sup>a</sup> Department of Immunology, Leiden University Medical Center, Leiden, the Netherlands

<sup>b</sup> Immunetune BV, Leiden, the Netherlands

<sup>c</sup> Synvolux Therapeutics BV, Leiden, the Netherlands

### ARTICLE INFO

#### Article history:

Received 29 July 2021

Received in revised form 10 January 2022

Accepted 4 February 2022

Available online 15 February 2022

#### Keywords:

DNA vaccination

Caspase-1

Cancer immunotherapy

Pyroptosis

### ABSTRACT

Pyroptosis is a recently discovered form of inflammatory programmed necrosis characterized by caspase-1-mediated and gasdermin D-dependent cell death leading to the release of pro-inflammatory cytokines such as Interleukin-1 beta (IL-1 $\beta$ ). Here, we evaluated whether pyroptosis could be exploited in DNA vaccination by incorporating a constitutively active variant of caspase-1 to the antigen-expressing DNA. *In vitro*, transfection with constitutively active caspase-1 DNA induced pro-IL-1 $\beta$  maturation and IL-1 $\beta$  release as well as gasdermin D-dependent cell death. To test active caspase-1 as a genetic adjuvant for the induction of antigen-specific T cell responses, mice were vaccinated intradermally with a DNA vaccine consisting of the active caspase-1 plasmid together with a plasmid encoding an ovalbumin-derived CD8 T cell epitope. Active caspase-1 accelerated and amplified antigen-specific CD8 T cell responses when administered simultaneously with the DNA vaccine at an equimolar dose. Moreover, upon challenge with melanoma cells expressing ovalbumin, mice vaccinated with the antigen vaccine adjuvanted with active caspase-1 showed significantly better survival compared to the non-adjuvanted group. In conclusion, we have developed a novel genetic adjuvant that for the first time employs the pyroptosis pathway to improve DNA vaccination against cancer.

© 2022 The Authors. Published by Elsevier Ltd. This is an open access article under the CC BY license (<http://creativecommons.org/licenses/by/4.0/>).

### 1. Introduction

Effective cancer vaccines require the induction of potent cancer-specific T cell immune responses. DNA vaccines represent a flexible platform allowing the inclusion of several well-defined tumor epitopes in a string-of-beads fashion. In mice, such DNA cancer vaccines generated tumor-specific immune responses able to eradicate the corresponding tumors [1–4]. Following these successful preclinical studies [5], several clinical trials established the safety and tolerability of plasmid DNA vaccines, as well as their ability to elicit T cell responses [6,7]. However, these T cell responses were often short-lived and very few studies demonstrated an improved clinical outcome [8,9].

In order to improve the immunogenicity of DNA vaccines in humans, defined adjuvants can be used to provide additional immune stimulation. Genetic adjuvants are DNA-encoded immune stimulatory proteins that can be delivered as an additional gene contained within the antigen-expressing DNA plasmid or as a separate plasmid mixed with the DNA vaccine. A detailed molecular understanding of the mechanisms underpinning effective antitumoral immune responses has inspired the development of several genetic adjuvants. These include immunomodulatory cytokines, chemokines, co-stimulatory [10] and adhesion molecules [11], aimed at inducing recruitment and maturation of dendritic cells or at improving T cell co-stimulation [12,13]. Indeed, DNA plasmids coding for different cytokines and chemokines such as GM-CSF, IL-12, IL-2, CCL5, CCL21 administered as an adjuvant improved immunogenicity and provided better tumor protection [14–18]. Thus, the inclusion of genetic adjuvants can shape the magnitude and the quality of vaccine-induced innate and adaptive immune responses.

\* Corresponding authors.

E-mail addresses: [F.A.Ossendorp@lumc.nl](mailto:F.A.Ossendorp@lumc.nl) (F. Ossendorp), [j.vanbergen@immunetune.com](mailto:j.vanbergen@immunetune.com) (J. van Bergen).

<sup>1</sup> These authors contributed equally.

<sup>2</sup> shared senior authors.

Recently, the molecular and cellular mechanisms by which the widely used adjuvant alum amplifies immune responses were uncovered [19,20]. Alum consists of aluminum salt crystals that induce endogenous danger signals responsible for inflammasome activation and the release of IL-1 $\beta$  and IL-18 cytokines [19,20]. In addition, they cause inflammatory tissue damage and necrosis of the muscle fibers at the immunization site, triggering the release of danger-associated molecular patterns (DAMPs) [21]. A key candidate pathway for the release of these cytokines and DAMPs is pyroptosis, a recently identified inflammatory form of programmed necrotic cell death [22,23]. The pyroptosis pathway has not yet been employed to design genetic adjuvants.

Microbial and non-infectious stimuli trigger pyroptosis by the activation of either the canonical or the non-canonical inflammasome pathway. It differs from other forms of cell death by the cleavage of gasdermin D by caspase-1 (canonical inflammasome pathway) or caspase-11 (non-canonical inflammasome pathway). In the canonical pathway, when pathogen-associated molecular patterns (PAMPs) and DAMPs activate their corresponding inflammasome sensors, the different signaling pathways converge on the recruitment of the central player pro-caspase-1. Through its non-catalytic Caspase Activation and Recruitment Domain (CARD) domain, pro-caspase-1 interacts with the upstream adaptors of the inflammasome pathway to form a supramolecular complex. By proteolytic autocleavage, pro-caspase-1 is activated releasing the CARD domain and active caspase-1 is released from the inflammasome assembly [24]. This autocleavage results in the unmasking of the active site cysteine in the activated caspase-1 catalytic domain which is composed of the 2 subunits p10 and p20 [20,25]. Activated caspase-1 then catalyzes the maturation of cytosolic cytokine precursors that do not possess secretion signals such as IL-1 $\beta$ , IL-18 and IL-33 [26,27] as well as the maturation of gasdermin D [28]. When caspase-1 has cleaved gasdermin D, its N-terminal domains are recruited to the cytoplasmic membrane to form pores through which cytokines as well as caspase-1 supramolecular complexes [29] can be released. Eventually the cell membrane is ruptured, causing pyroptotic cell death [28,30,31]. In this study, we describe the construction of a constitutively active caspase-1 DNA and investigate its efficiency as a genetic adjuvant to improve DNA vaccination against cancer.

## 2. Results

### 2.1. Design of constitutively active caspase-1 DNA

Given its central role in the pyroptosis pathway [32], we decided to design a constitutively active form of caspase-1 as a putative adjuvant. This design was inspired by previous studies, in which constitutively active caspase-3, caspase-6 and caspase-14 were generated by switching the order of their large (p20) and small (p10) subunits [33,34]. In addition to switching these domains, the caspase-1 sensitive cleavage site from IL-1 $\beta$  was added between p10 and p20 domains to facilitate their autocatalytic separation (Fig. 1a, [supplementary Table 1](#)). Furthermore, as active caspase-1 (Casp1\_active) should be active independently of upstream inflammasome activation, the CARD domain linking it to the key adaptor protein Asc (Apoptosis-associated speck-like protein containing a CARD) was removed. In order to study the requirement for the catalytic site in the caspase-1 p20 domain in the active caspase-1, we designed a second construct (Casp1\_inactive) with a single Cysteine (C) to Glycine (G) mutation in the p20 catalytic domain (C305 in Casp1 active, corresponding to C284 in wild-type caspase-1) (Fig. 1a; [supplementary Table 1](#)). Finally, a construct encoding wild-type caspase-1 (Casp1\_WT), which does

require the activation of the upstream inflammasome pathway to become functional, was included.

To characterize the products of the different DNA constructs, 293 cells were transfected with the caspase-1 plasmids. Transfected cells were either left untreated or were treated with Z-VAD-FMK (a cell permeable potent pan-caspase inhibitor binding irreversibly to the active site) in order to retain caspase-1 intracellularly in its intact form by inhibiting its activation and its release. An antibody against the p20 subunit detected WT caspase-1 as well as inactive caspase-1 in cell lysates at their expected molecular weights independently of the Z-VAD-FMK treatment. In contrast, active caspase-1 was detectable only after treating cells with Z-VAD-FMK ([supplementary Fig. 1a](#)). These data suggested that, like inflammasome-activated caspase-1, active caspase-1 undergoes autoproteolysis and is subsequently released from cells in an active-site-dependent manner.

### 2.2. Active caspase-1 mediates pro-IL-1 $\beta$ processing and IL-1 $\beta$ release via its enzymatically active site

Caspase-1 cleavage activity is required for the maturation of the precursors of the pyrogenic cytokine pro-IL-1 $\beta$  into mature IL-1 $\beta$  [35]. We therefore tested whether active caspase-1 is able to process pro-IL-1 $\beta$  and release the IL-1 $\beta$  cytokine from the cells. To this end, B16-F10 cells were co-transfected with either a control plasmid (-) or a pro-IL-1 $\beta$  plasmid (*pro-IL-1 $\beta$  DNA*) mixed together with the different variants of caspase-1 plasmids ([supplementary Table 1](#)), and IL-1 $\beta$  release was quantified by ELISA. When co-transfected with pro-IL-1 $\beta$  plasmid, only active caspase-1, but not WT caspase-1 or inactive caspase-1, induced IL-1 $\beta$  release from B16-F10 cells (Fig. 1b). As co-transfection of pro-IL-1 $\beta$  with the N-terminal domain of GSDMD (*Gsdmd\_N-ter*), which induces membrane pores to allow cytokine release, did not result in detectable IL-1 $\beta$  release (Fig. 1b), it is unlikely that unprocessed pro-IL-1 $\beta$  was responsible for this signal. When co-transfected with mature, caspase-1 independent IL-1 $\beta$  (*mature IL-1 $\beta$  DNA*) instead of pro-IL-1 $\beta$ , B16-F10 cells released IL-1 $\beta$  cytokine irrespective of the different caspase-1 variants ([supplementary Fig. 1b](#)). These data show that active caspase-1 can induce pro-IL-1 $\beta$  processing and IL-1 $\beta$  release, and that this is dependent on its enzymatically active site in the p20 subunit.

### 2.3. Active caspase-1 induces gasdermin D-dependent cell death, but does not prevent antigen expression

In addition to processing pro-IL-1 $\beta$  into its active form, active caspase-1 can also cleave gasdermin D to release its N-terminal domain, which subsequently forms pores in the cell membrane by oligomerization to induce pyroptotic death [28,36]. To evaluate the capacity of the active caspase-1 to promote pyroptotic cell death, 293 cells were co-transfected with either a control plasmid (-) or wild-type gasdermin D (*Gsdmd\_WT DNA*), together with the different variants of caspase-1 plasmids or the N-terminus of gasdermin D (*Gsdmd\_N-ter*). Lactate dehydrogenase (LDH) release in the culture medium was determined as a measure of cell death. When co-transfected with WT *Gsdmd*, active, but not WT or inactive caspase-1, induced LDH release (Fig. 1c). LDH leakage was not observed when *Gsdmd\_WT* was replaced with a control plasmid, demonstrating that active caspase-1 induces gasdermin D-dependent and therefore pyroptotic cell death.

As pyroptotic cell death might limit antigen expression in a vaccination setting, we next assessed whether cells undergoing active caspase-1-induced pyroptotic cell death express model antigen GFP. Two days after transfection with the caspase-1 constructs, cell death (7-AAD) and antigen expression (GFP) were analyzed by flow cytometry. In contrast with WT caspase-1, active caspase-1

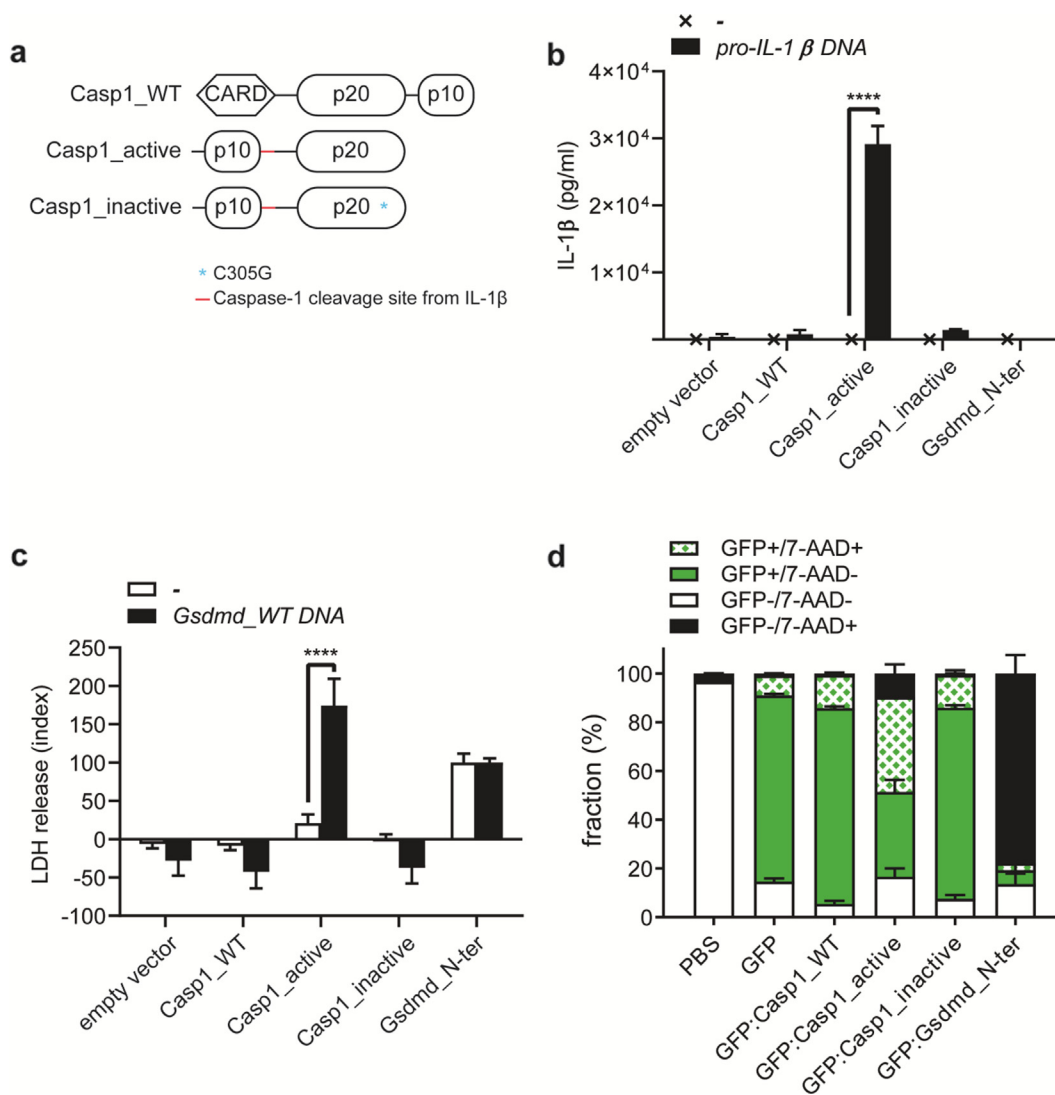


**Fig. 1. Active caspase-1 induces pro-IL-1 $\beta$  processing, IL-1 $\beta$  secretion and cell death *in vitro*.** **a** Schematic representation of the different caspase-1 constructs. The expected molecular weights of the resulting proteins are indicated on the right of each construct. **b** Quantification of IL-1 $\beta$  in the supernatant of transfected cells by ELISA. B16-F10 cells were co-transfected with either a control plasmid (-) or a pro-IL-1 $\beta$  plasmid (pro-IL-1 $\beta$  DNA) mixed with the different caspase-1 DNA constructs. Two days after transfection, supernatants were harvested for IL-1 $\beta$  quantification. Data are mean  $\pm$  SEM from 5 independent experiments. **c** Quantification of LDH release in the supernatant of transfected cells using LDH assay. 293 cells were co-transfected with either a control plasmid (-) or a wild-type gasdermin D plasmid (Gsdmd\_WT DNA) together with the different caspase-1 DNA constructs. Two days after transfection, supernatants were harvested for LDH release quantification. Data are normalized to control plasmid and Gsdmd\_N-ter DNA transfected conditions. Data are mean  $\pm$  SEM from 3 independent experiments. **d** Percentage of the different live/dead cell populations set at 0 and 100, respectively, expressing or not GFP as a model antigen after co-transfection with the different caspase-1 DNA constructs. B16-F10 cells were transfected with the indicated DNA constructs mixed with GFP encoding plasmid. Two days after transfection, cells were harvested and stained with 7-AAD. The PBS-treated group served as a negative control for transfection, and the GFP group as a baseline for cell death, while the GFP:Gsdmd\_N-ter served as positive control for cell death. In **b** and **c**, statistical difference was determined using two-way ANOVA followed by Sidak's multiple comparisons test; \*\*\*\*  $p < 0.0001$ . When statistical significance is not indicated, significance levels were  $> 0.05$ .

induced significant cell death, while the N-terminal domain of gasdermin D killed nearly all B16-F10 cells (Fig. 1d). However, in contrast with latter, the large majority of cells killed by active caspase-1 were positive for GFP (Fig. 1d), indicating that pyroptotic cell death induced by active caspase-1 does not prevent antigen expression.

#### 2.4. Active caspase-1 increases functional antigen-specific T cell responses in a dose-dependent manner

As the constitutively active caspase-1 DNA mimicked inflammasome activation by inducing IL-1 $\beta$  secretion and pyroptotic cell death *in vitro*, we studied *in vivo* its potential as a genetic adjuvant for our previously developed DNA vaccine [37]. To determine

whether active caspase-1 DNA can improve antigen-specific T cell responses, we injected mice intradermally with antigen-expressing DNA supplemented with different doses of active caspase-1 DNA (Fig. 2a). The antigen-expressing DNA included two model antigens derived from ovalbumin, the H2-K<sup>b</sup>-restricted CD8<sup>+</sup> T cell epitope SIINFEKL and the I-A<sup>b</sup>-restricted CD4<sup>+</sup> T cell epitope ISQAVHAAHAEINEA, as well as three tumor-specific neoantigens (Dpagt1, Repts1, Adpgk) derived from the C57BL/6 MC38 colon carcinoma cell line [38]. Tracking SIINFEKL-specific CD8<sup>+</sup> T cell responses in blood using tetramers (Fig. 2b) indicated that at a 1:1 antigen:adjuvant (10  $\mu$ g each) ratio, active caspase-1 improved this T cell response both after prime (d0) and boost (d38) vaccinations. Shortly after the first vaccination (d6), this difference was statistically significant (Fig. 2c). In contrast, five-fold lower (2  $\mu$ g

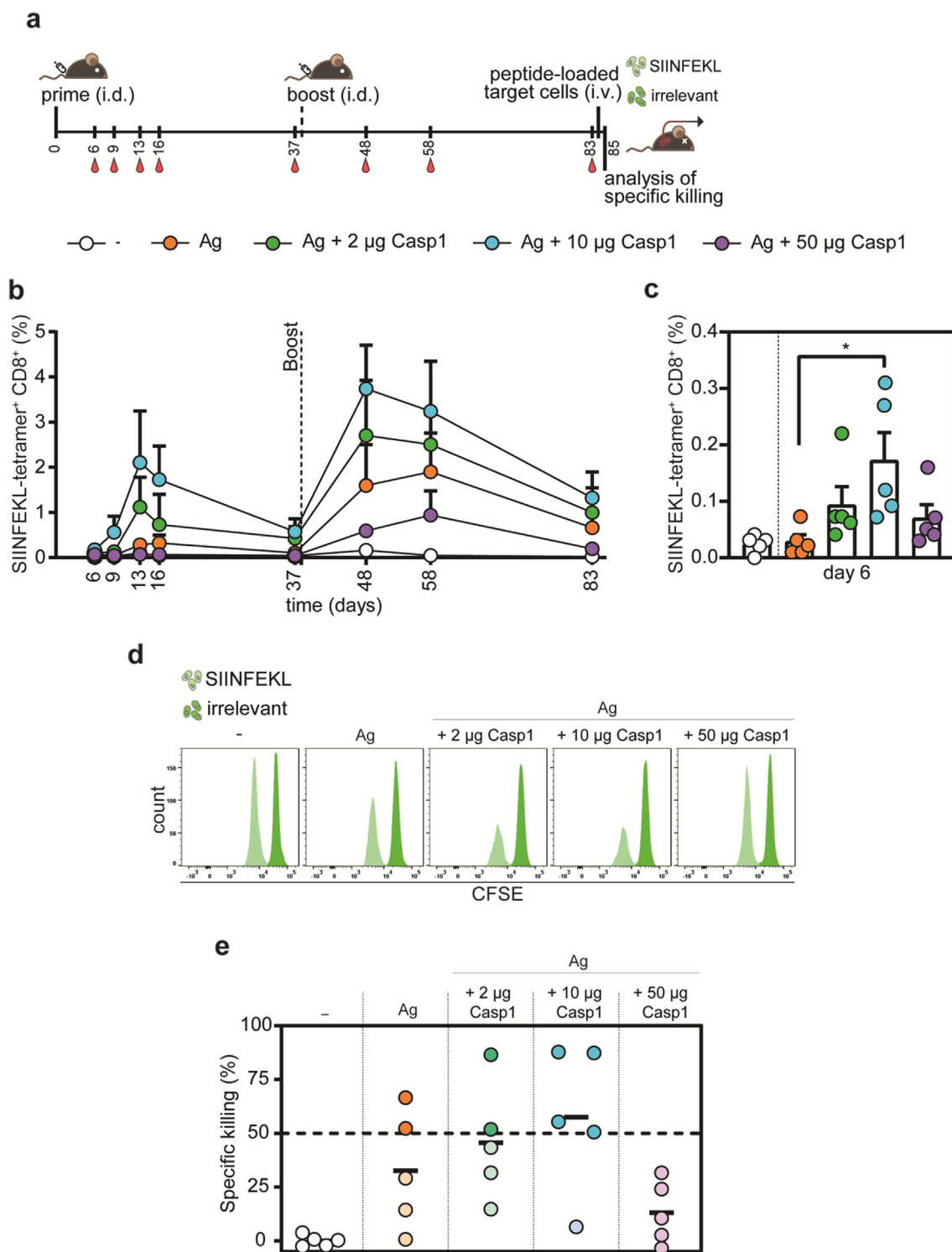


**Fig. 2. Active caspase-1 improves functional T cell responses in a dose-dependent manner.** **a** Schematic overview of the vaccination experiment. C57BL/6 mice were primed (day 0) and then boosted (day 28) intradermally (i.d.) at the tail base with either a control plasmid (-), antigen-DNA alone (Ag) or antigen-DNA adjuvanted with 2 µg, 10 µg or 50 µg of active caspase-1 (Ag + Casp1). On different days, SIINFEKL-specific CD8 T cells were monitored in blood by flow cytometry. On day 83, mice were injected with CFSE-labelled SIINFEKL-loaded target cells and specific killing was analyzed 2 days later. **b** Kinetics of SIINFEKL-specific T cells monitored in blood over time. Data are reported as average percentage of total CD8<sup>+</sup> T cells (n = 5 mice/group). **c** Percentage of SIINFEKL-specific CD8<sup>+</sup> T cells in blood 6 days after vaccination. **d** Representative flow cytometry histograms of detected CFSE-labelled target cells loaded either with an irrelevant peptide (CFSE high) or with SIINFEKL peptide (CFSE low) detected in the spleens of the vaccinated mice. **e** Specific killing of peptide-loaded target cells (n = 5 mice/group). In panels **b** and **c**, error bars indicate mean ± SEM. In figure **c**, statistical significance was determined using the Kruskal-Wallis test followed by Dunn's multiple comparison test (compared to Ag group); \*p < 0.05.

or higher (50 µg) amounts of active caspase-1 adjuvant only marginally increased or decreased, respectively, the SIINFEKL-specific T cell response compared to the non-adjuvanted vaccine (Fig. 2b,

2c). In conclusion, these data indicate that active caspase-1 amplifies antigen DNA-induced T cell responses, and that the optimal antigen:adjuvant DNA ratio is approximately 1:1.

To assess the functionality of the vaccine-induced CD8 T cells, mice were injected intravenously with CFSE-labeled target cells loaded either with SIINFEKL (CFSE low) or an irrelevant (CFSE high) epitopes (Fig. 2a). Compared to mock-vaccinated mice, mice receiving antigen coding DNA specifically eliminated SIINFEKL-loaded but not control cells (Fig. 2d, 2e). In line with the tetramer data (Fig. 2b, 2c), the *in vivo* killing of SIINFEKL-loaded target cells appeared most pronounced at a 1:1 antigen:adjuvant ratio (10 µg adjuvant), while five-fold lower (2 µg) or higher (50 µg) amounts of caspase-1 adjuvant slightly increased or decreased, respectively, the antigen-specific killing compared to the non-adjuvanted vaccine (Fig. 2e). Altogether these data show that DNA vaccine elicits functional cytolytic CD8 T cells, and indicate that at an optimal antigen:adjuvant DNA ratio, active caspase-1 improves this response.

### 2.5. Vaccination with active caspase-1 DNA reduces expression of model antigen luciferase in a dose-dependent manner

Since at its highest dose, active caspase-1 appeared to reduce rather than increase vaccine-induced T cell responses (Fig. 2), and since active caspase-1 can induce pyroptosis (Fig. 1d), we speculated that death of antigen-expressing cells might limit adjuvant efficacy at a supra-optimal dose. To explore this issue, we tested the 3 different doses (2 µg, 10 µg and 50 µg) of active caspase-1 (Casp1) DNA mixed with a fixed amount (10 µg) of DNA encoding luciferase gene (Luc-Ag), which was used as a traceable model antigen (supplementary Table 2). Upon intradermal injection of this mixture, live bioluminescence imaging of the mice allowed the tracing of luciferase protein expression at the vaccination site and loss of luminescent signal as an indirect measure of cell death. Six days after vaccination, we detected marginally lower luciferase expression levels in the groups adjuvanted with 2 µg and 10 µg active caspase-1 compared to the non-adjuvanted mice (Fig. 3a–b). However, vaccinating with 50 µg of active caspase-1 resulted in significantly lower luciferase expression levels compared to Luc-Ag alone (Fig. 3a–b). As time progressed, also the lower adjuvant doses reduced luciferase expression levels compared to the non-adjuvanted group (Fig. 3c). These data demonstrate that active caspase-1 is indeed able to reduce expression of a model antigen *in vivo*, most likely by inducing death and antigen release of antigen-expressing cells. Based on these results (Figs. 2–3), a 1:1 antigen:adjuvant plasmid ratio (10 µg of each plasmid DNA) was chosen for subsequent experiments.

### 2.6. Active caspase-1 improves T cell responses optimally when administered simultaneously with DNA vaccine

As active caspase-1 reduced antigen expression, particularly at a high dose (Fig. 3), we hypothesized that delaying the administration of the caspase-1 DNA might improve the efficacy of this adjuvant, as cells would only die after building up sufficient antigen. To determine the optimal timing of active caspase-1 DNA administration, mice were primed with the antigen-coding DNA (day 0) while the active caspase-1 DNA was administered at the same site either one day prior to vaccination (day –1), on the same day (day 0), or one (day + 1) or three (day + 3) days after vaccination (Fig. 4a). All mice were then boosted with the antigen DNA only (day 38). At several days post-vaccination, SIINFEKL-specific CD8 T cell frequencies in blood were determined by flow cytometry (Fig. 4a, 4b). On day 13, active caspase-1 administered together with the antigen DNA greatly increased the frequency of SIINFEKL-specific T cells, while caspase-1 injected before (day –1) or after (day + 1, +3) the antigen DNA had no effect (Fig. 4c). Also at the other time points measured, delayed administration of caspase-1 did not improve T cell responses compared to simultaneous

administration (Fig. 4d). Based on these results, we concluded that the active caspase-1 DNA is best administered simultaneously with the antigen-coding DNA.

### 2.7. Active caspase-1 accelerates and amplifies DNA vaccine-induced T cell responses

Using the optimized dosing and timing of active caspase-1 DNA administration, we performed several immunization experiments in which we tracked SIINFEKL-specific and Adpgk-specific CD8 T cells levels in blood for several days post-vaccination (Fig. 5a). On day 0, mice were vaccinated with either a control plasmid, 10 µg antigen DNA vaccine alone (Ag) or adjuvanted with 10 µg active caspase-1 DNA (Ag + Casp1). From day 6 to day 27 post-vaccination, antigen DNA vaccinated groups, either adjuvanted with active caspase-1 or not, showed SIINFEKL-specific T cell responses (Fig. 5b). Moreover, from day 6 to day 13 post-vaccination, active caspase-1 significantly (up to 8-fold) improved these antigen-specific T cell responses compared to the non-adjuvanted group (Fig. 5b, 5c). Vaccine-induced Adpgk-specific CD8 T cells levels in blood were much lower compared to SIINFEKL-specific T cells. Despite this, we did detect a positive effect of active caspase-1 on vaccine-induced Adpgk-specific CD8 T cell responses (supplementary Fig. 2). Importantly, the kinetics of this effect corresponded to those observed with the CD8 T cell epitope SIINFEKL (supplementary Fig. 2). Based on these results, we concluded that constitutively active caspase-1 amplifies the antigen-specific T cell response compared to non-adjuvanted group as early as 6 days post-vaccination.

### 2.8. Active caspase-1 improves CD8 T cell responses and increases survival of mice upon challenge with tumor cells

As addition of the active caspase-1 adjuvant to the antigen-coding DNA vaccine significantly increased the frequency of antigen-specific T cells, we analyzed the potential of active caspase-1 as a genetic adjuvant in a tumor control study. To this end, mice were vaccinated with antigen DNA mixed either with active caspase-1 or a control plasmid. At several time points post-vaccination, SIINFEKL-specific T CD8 T cells were quantified in blood by flow cytometry, and on day 28 post-vaccination, mice were challenged with B16-OVA tumor cells and tumor outgrowth was monitored (Fig. 6a). At all time points measured, including two weeks after tumor challenge, the active caspase-1 adjuvanted group (Ag + Casp1) showed a significantly higher percentage of SIINFEKL-specific T cells compared to the non-adjuvanted group (Ag) (Fig. 6b). In mock-vaccinated mice, B16-OVA tumors grew out within three weeks after injection (Fig. 6c, left panel; Fig. 6d). Although the antigen-coding DNA vaccine significantly delayed tumor growth (Fig. 6c, middle panel; Fig. 6d), only 19% of the mice (3 of 16 mice) remained tumor-free (Fig. 6c, middle panel; 6e). In contrast, 56% of active caspase-1 adjuvanted mice (9 of 16 mice) remained tumor-free (Fig. 6c, right panel; Fig. 6d) and 3 additional mice had an increased survival time (Fig. 6d). Thus, the constitutively active form of caspase-1, used as adjuvant in a DNA vaccine, significantly improved both T cell immunity and tumor control.

## 3. Discussion

In this study, we exploited pyroptotic cell death as a novel strategy to enhance T cell response induction by DNA vaccination against cancer antigens. Therefore, we designed a constitutively active caspase-1, the central player of the pyroptosis pathway, by switching the order of their p20 and p10 subunits. *In vitro* cell

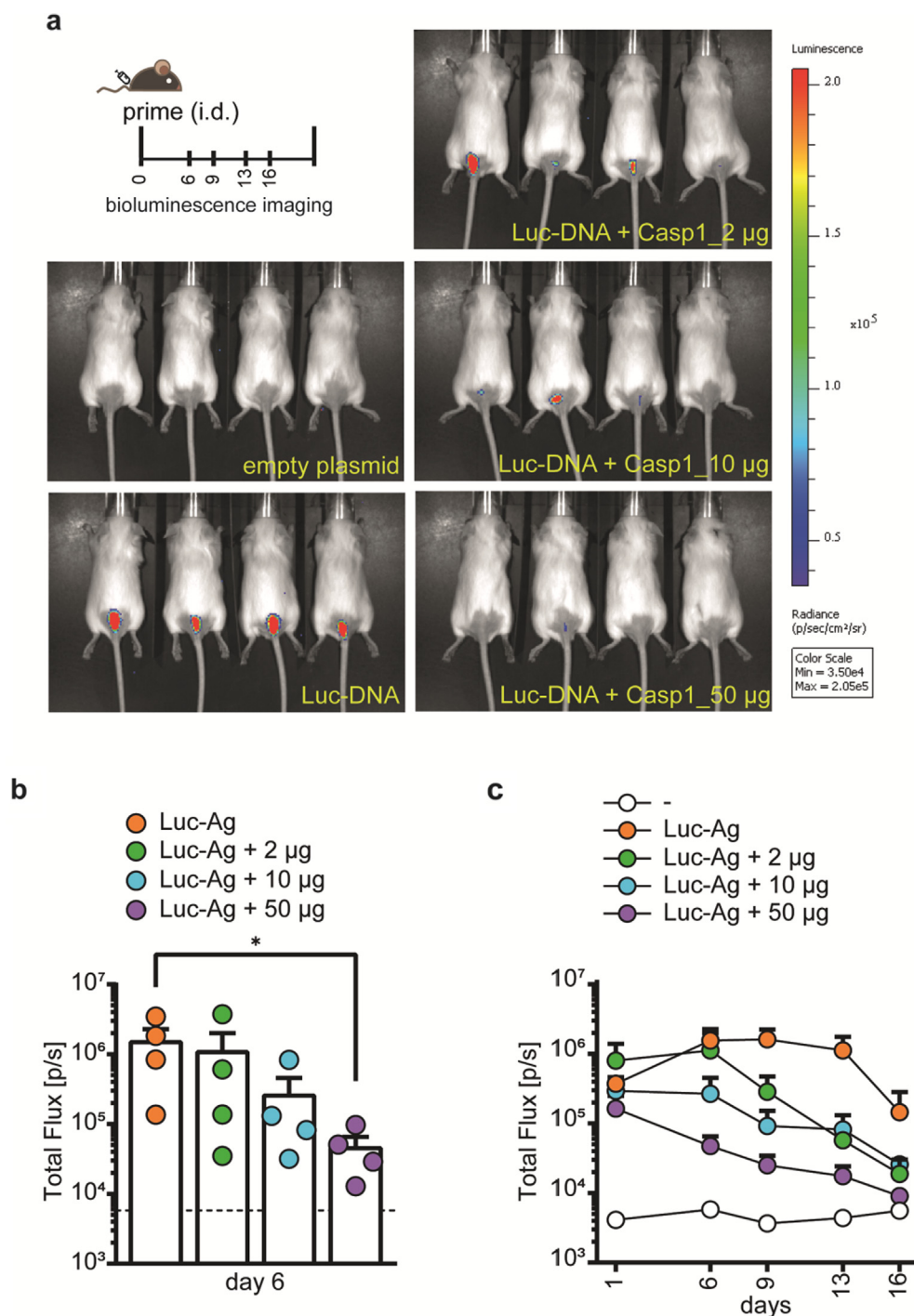


**Fig. 3. Active caspase-1 limits antigen expression *in vivo* in a dose-dependent manner.** **a** Mice were vaccinated with 10 µg of DNA including luciferase gene (Luc-Ag) alone or in combination with 2 µg, 10 µg or 50 µg of active caspase-1 DNA. The expression of the luciferase at the tail base was monitored over 16 days. Representative bioluminescence intensity (BLI) images 6 days after intradermal DNA vaccination at the tail base are shown. **b** Quantification of the luciferase signal at the tail base 6 days after vaccination. **c** Kinetics of BLI resulting from luciferase expression (gated on the injected site) of the DNA vaccination without or with different doses of active caspase-1. Data are the average  $\pm$  SEM of 4 mice per group. The negative group was injected with 20 µg control plasmid. In figure **b**, statistical significance was determined using Kruskal-Wallis test followed by Dunn's multiple comparison test (compared to Luc-Ag group); \* $p < 0.05$ .

transfection studies with active caspase-1 showed the induction of the maturation and release of IL-1 $\beta$ , as well as gasdermin D-dependent cell death without preventing antigen expression. *In vivo* studies showed that mixing constitutively active caspase-1 with the antigen DNA vaccine accelerated and amplified the induction of antigen-specific CD8 T cells in a dose-dependent manner. Increasing amounts of active caspase-1 DNA reduced expression

of a co-injected reporter luciferase construct, suggesting that caspase-1 indeed induces cell death at the site of vaccination. After being challenged with tumor cells, mice which were vaccinated with active caspase-1 adjuvanted antigen DNA showed significant delay in tumor growth and increased survival.

While wild-type caspase-1 requires upstream inflammasome signaling in order to be processed and activated, this novel adju-

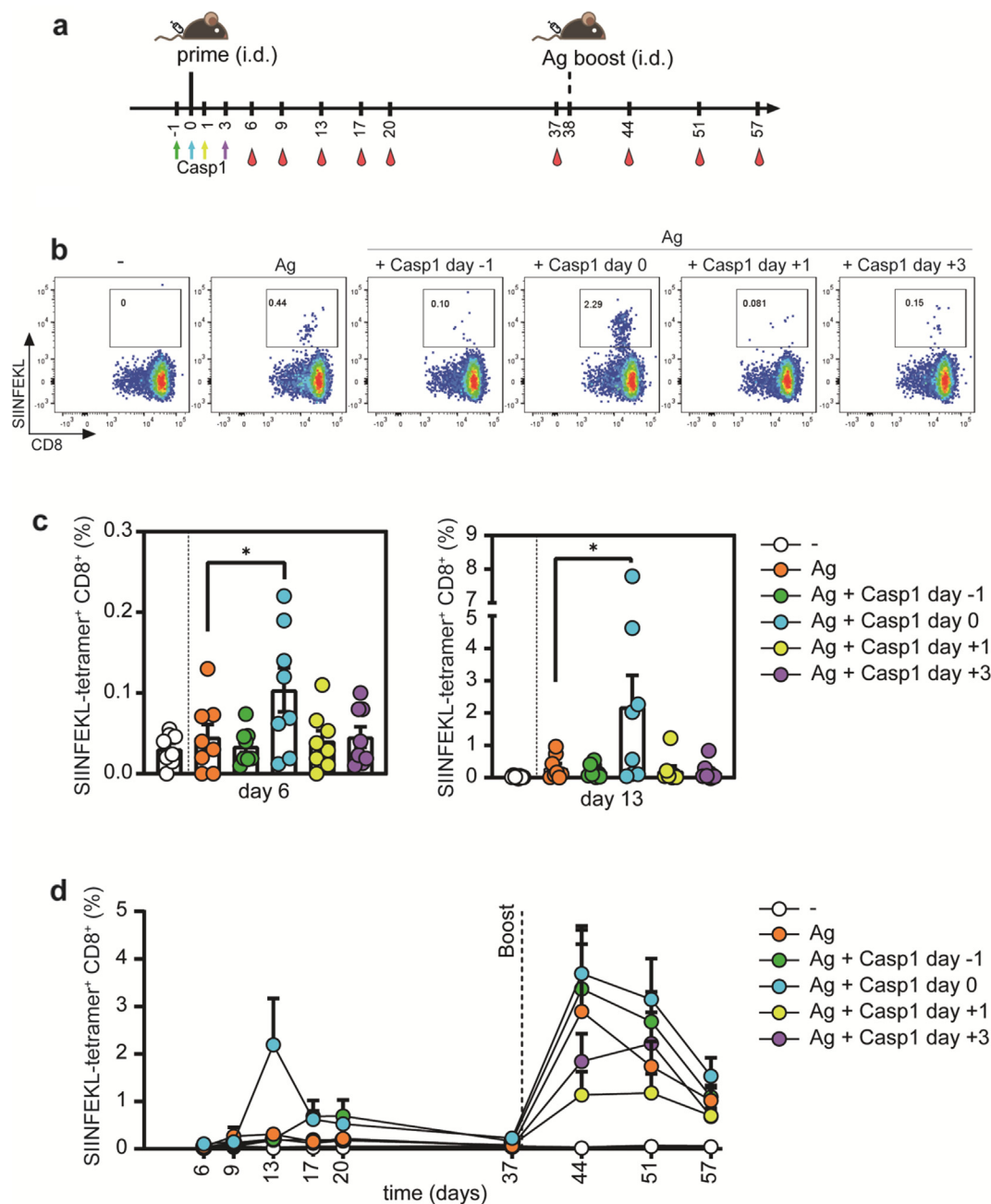


**Fig. 4. Active caspase-1 improves T cell responses when administered simultaneously with DNA vaccine.** **a** Schematic overview of the vaccination experiment including the vaccine administration and tetramer staining schedule in C57BL/6 mice. Mice were primed intradermally with either a control plasmid (-) or with the antigen-DNA on day 0. They received 10  $\mu$ g active Casp1 either together with the antigen-DNA (Ag + Casp1 day 0), one day prior to priming (Ag + Casp1 day -1), one day later than priming (Ag + Casp1 day +1) or three days later than priming (DNA + Casp1 day +3). Mice were boosted intradermally at the tail base with the antigen-DNA alone (day 38). On different days, SIINFEKL-specific CD8<sup>+</sup> T cells were monitored in blood by flow cytometry. **b** Representative dot plots of SIINFEKL-specific CD8<sup>+</sup> T cells on day 13. **c** Percentage of SIINFEKL-specific T cells in blood 6 and 13 days after vaccination. **d** Kinetics of SIINFEKL-specific T cells monitored in blood over time and measured by SIINFEKL-H2-K<sup>b</sup> tetramer staining. Data are reported as average percentage of total CD8<sup>+</sup> T cells (n = 8 mice/group). Error bars indicate mean  $\pm$  SEM. In panel c, statistical significance was determined using the Kruskal-Wallis test followed by Dunn's multiple comparison tests (compared to Ag group); \*p < 0.05.

vant is constitutively active and able to induce IL-1 $\beta$ /gasdermin D processing independently of upstream events. By uncoupling caspase-1 from upstream signaling, it has become a reliable mimic of inflammasome activation, unaffected by biological variation between cells or individuals. Using a constitutively active version of an inflammatory mediator as a genetic vaccine adjuvant is not without precedent: this principle has been applied previously to activate the RIG-I/MDA-5 [39] and cGAS/STING pathways [40,41]. We therefore tested active caspase-1, but not its wild-type counterpart, as a potential genetic adjuvant.

Since a high dose of active caspase-1 DNA did not increase the frequency of antigen-specific T cells nor enhanced killing capacities, the timing of cell death and the level of antigen expression may be closely linked. We hypothesize that there is a minimum threshold for sufficient expression of the antigens encoded by the antigen expressing DNA to be reached before the induction of pyroptotic cell death can increase immunogenicity. This hypothesis is supported by several studies in which cell death-inducing molecules were tested in DNA vaccination and the importance of timing and the strength of the promoter of the adjuvant plasmid

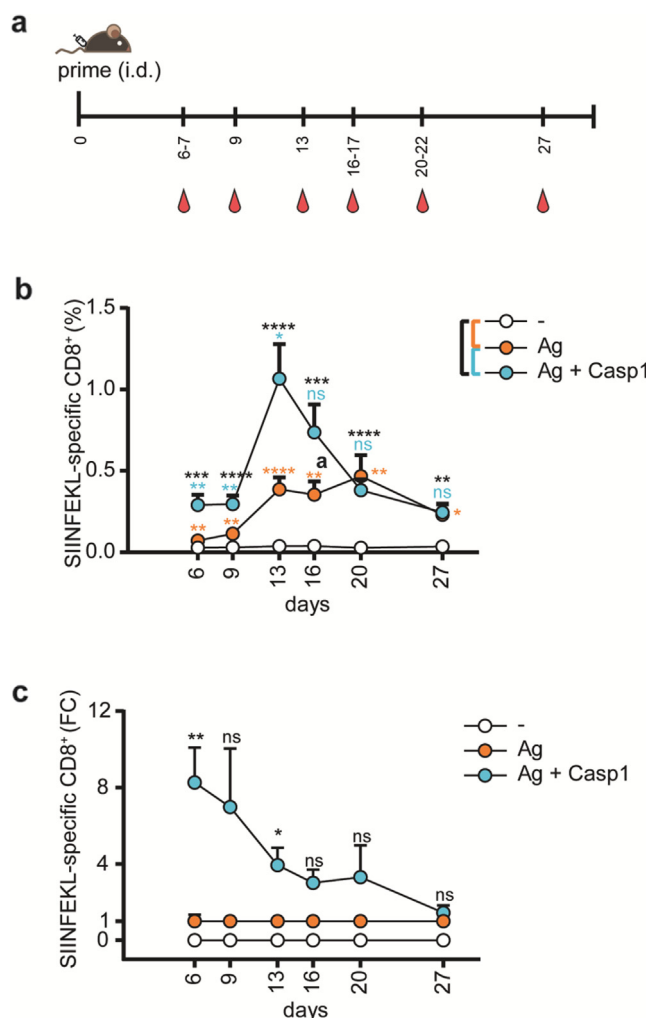


**Fig. 5. Active caspase-1 accelerates and amplifies T cell responses induced by DNA vaccination.** **a** Schematic overview of the vaccination experiment including the vaccine administration and tetramer staining schedule in C57BL/6 mice. C57BL/6 Mice were primed intradermally with either a control plasmid (-), 10  $\mu$ g of antigen DNA alone (Ag) or adjuvanted with 10  $\mu$ g of active caspase-1 (Ag + Casp1). On different days, SIINFEKL-specific CD8<sup>+</sup> T cells were monitored in blood by flow cytometry. **b** Kinetics of SIINFEKL-specific T cells monitored in blood over time. Data represent 9 independent experiments with 3–10 mice per group, including the experiments shown in Figs. 2, 4 and 6, and each individual data point is the average of at least 3 experiments. Error bars indicate mean  $\pm$  SEM. **c** SIINFEKL-specific T cells in blood normalized to antigen-vaccinated group and reported as fold change (FC) on days 6/7 (n = 42–49), days 9/10 (n = 55–64), day 13 (n = 47–56), days 16/17 (n = 28–33), days 20, 21, 22 (n = 26–33) and day 27 (n = 22–25). In **b** and **c**, statistical significance was determined using two-way ANOVA followed by Sidak's multiple comparison test. \*p < 0.05; \*\*p < 0.01; \*\*\*p < 0.001; \*\*\*\*p < 0.0001; ns: not significant.

to induce functional T cell responses were reported [42,43]. Inducing necrosis in vaccine-transfected cells with a DNA encoding a viral antigen and the cytolytic protein perforin enhanced CD8 T cell responses to the antigen and reduced the viral load following challenge with the virus [42]. Also in this case, the immune enhancement was dependent on the timing of cell death after antigen expression [42]. In order to give some time for the antigen to be expressed, the active caspase-1 construct was delivered one or three days after DNA vaccination. However, this delayed timing strategy did not improve the frequency of antigen-specific T cells (Fig. 4a–d). This may be explained by inaccurate targeting of the active caspase-1 DNA to the antigen DNA transfected cells. Alternatively, the levels of *in vivo* transfection may not be sufficient after a first DNA vaccination. Therefore, for future studies, it would be

interesting to design a bicistronic construct encoding the antigen and the active-caspase-1 genes under different promoters or to use an inducible caspase-1 DNA system to test this hypothesis.

To determine which cells are being targeted *in vivo* by a DNA vaccine upon intradermal injection, further studies are required. Luciferase expression was detected only at the tail base, at the site of vaccination. Mechanistically, it is important to understand which cells are targeted by the DNA vaccine (skin cells, APCs), how antigens are released from the transfected cells and whether they are actively taken up by local APCs or they passively drain to the lymph nodes [44]. Even though active caspase-1 DNA was able to enhance T cell immune responses, its expression in the skin resident APCs is not desirable in order to avoid their death. In support of this notion, it has been shown that delivery of DNA encoding anti-apoptotic factors to the dendritic cells enhances antigen-specific immune responses by prolonging their life span [45]. Therefore it is likely that the pyroptotic mode of action of active caspase-1 in our model is occurring in dermal skin cells rather than in dendritic cells. Reportedly, intradermal injection of free DNA induces transfection and protein expression mainly in keratinocytes [46]. This suggests that antigen cross-presentation may be occurring after intradermal vaccination. However direct antigen presentation by APCs cannot be ruled out.

In addition to antigen release after pyroptotic cell death, several inflammatory cytokines are secreted as a result of gasdermin D pore formation and inflammatory cell death. It is likely that the potent inflammatory cytokines IL-1 $\beta$  and IL-18 also play a role in enhancing DNA vaccine-induced immunity. *In vitro*, active caspase-1 DNA was able to induce IL-1 $\beta$  processing and secretion (Fig. 1c). Several studies investigated different chemokines and cytokines and their immunostimulatory effects in DNA vaccination against pathogens [47–49]. Interestingly, administration of IL-1 $\beta$  or IL-18 either as DNA or peptide is shown to stimulate antigen-specific T cell responses [50–53]. In addition to IL-1 $\beta$  and IL-18, several low-molecular weight proinflammatory mediators such as HMGB1 and IL-1 $\alpha$ , soluble molecules like ATP are secreted in the extracellular matrix and contribute to the activation of innate and adaptive immune responses [54]. The involvement of these inflammatory factors in the amplification of T cell responses by the active caspase-1 adjuvant has yet to be determined.

Given the inflammatory nature of pyroptotic cell death, it is surprising that no significant side effects (inflammation or tissue damage) were observed at the vaccination site after intradermal injection, presumably because cell death was limited to the tail base area to DNA-vaccine transfected cells which can only transcribe and translate the DNA vaccine into functional protein products. Active caspase-1 DNA therefore appears to possess advantages regarding safety in comparison to the classical Alum adjuvant that also activates inflammasome pathway but causes local side effects [20,55].

In summary, our data demonstrate that constitutively active caspase-1, representative of a new class of genetic adjuvants, positively impacts DNA vaccination. Antigen expressing DNA adjuvanted with constitutively active caspase-1 resulted in increased induction of antigen-specific CD8 T cells and improved survival after a tumor challenge in a pre-clinical mouse model. Given the effectiveness of this approach, it will be worthwhile to evaluate whether this strategy can be translated to the clinic.

## 4. Materials and methods

### 4.1. Cell lines

The murine B16-F10 melanoma cell line was maintained in Iscove's Modified Dulbecco's Medium (Lonza, Walkersville, MD,

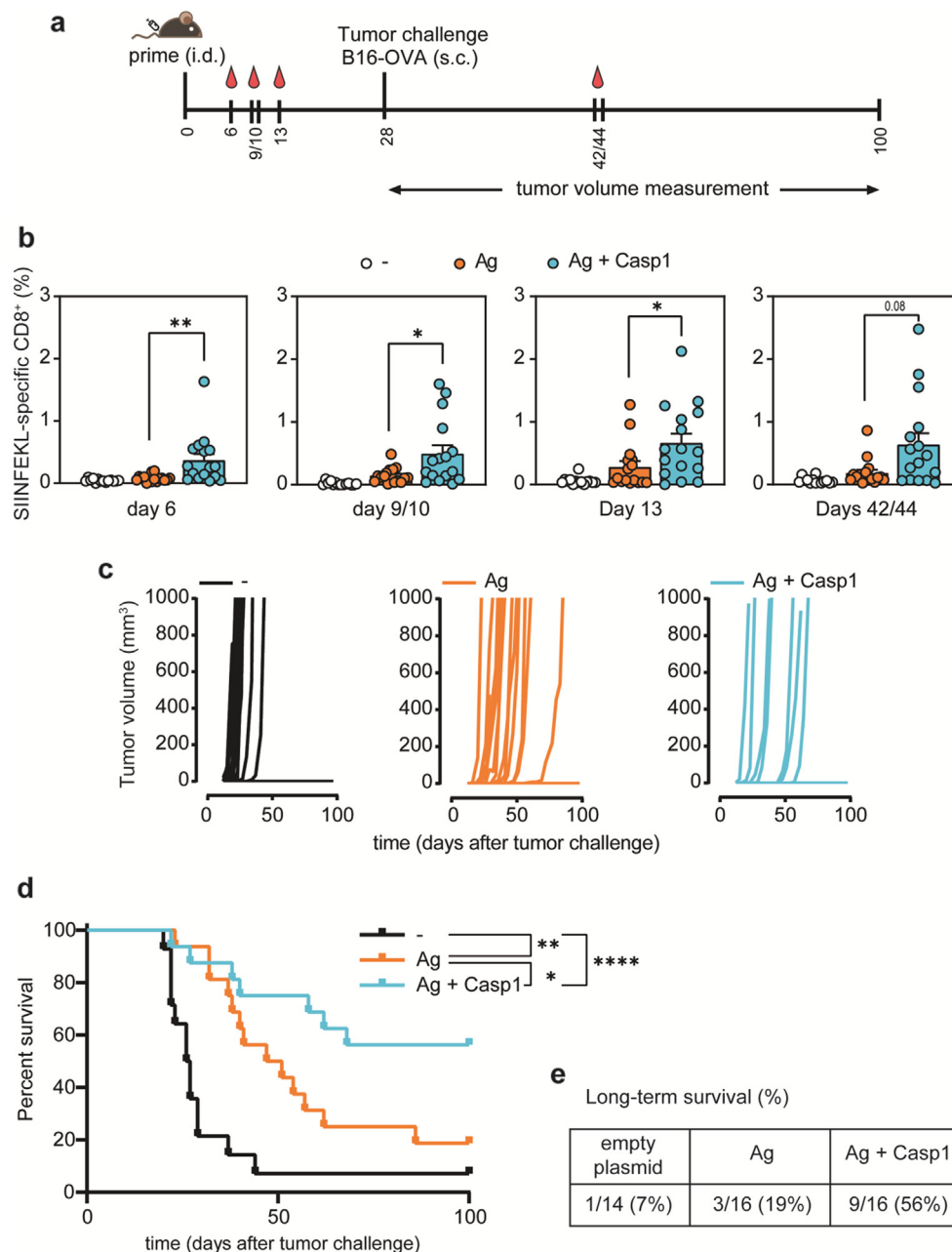


**Fig. 6. DNA vaccination with active caspase-1 protects against B16-OVA tumor growth and improves survival.** **a** Schematic overview of the prophylactic vaccination experiment. On day 0, mice were vaccinated intradermally (i.d.) at the tail base with either a control plasmid (-), 10 μg of antigen DNA alone (Ag) or adjuvanted with 10 μg of active caspase-1 (Ag + Casp1). On day 28, mice were challenged subcutaneously (s.c.) with 100,000 B16-OVA tumor cells on their flank. On several days, SIINFEKL-specific CD8<sup>+</sup> T cells were monitored in blood by flow cytometry. Tumor outgrowth was monitored and measured over time. Mice were euthanized when tumor volume had reached 1,000 mm<sup>3</sup> or when a humane endpoint was reached. **b** Percentage of SIINFEKL-specific T cells in blood on day 6, days 9/10, day 13 and days 42/44. **c** B16-OVA tumor growth curves (reported in mm<sup>3</sup>) of individual mice after tumor challenge in the control group (n = 14), antigen DNA vaccinated (n = 16) and adjuvanted with active caspase-1 (n = 16) groups. **d** Tumor-free survival of mice in the control group (-), in antigen DNA (Ag) or adjuvanted with active caspase-1 (Ag + Casp1) groups. **e** The number of mice (also reported as percentage) that were challenged subcutaneously with B16-OVA tumor cells and that remained tumor-free is shown. Data is the summary of 2 independent experiments. Statistical significance was determined using either Kruskal-Wallis test (panel b) or Log-rank Mantel-Cox test (panel d); \* p < 0.05; \*\* p < 0.01.

USA) supplemented with 8% fetal calf serum (Sigma-Aldrich), 2 mM L-glutamine, 50 IU/ml penicillin, 50 μg/ml streptomycin (all from Gibco, Life Technologies) and 30 μM β-mercaptoethanol (Merck Millipore) in a humidified CO<sub>2</sub> incubator (37 °C, 5% CO<sub>2</sub>). The B16-OVA cell line was maintained in B16-F10 culture medium supplemented with non-essential amino acids, sodium pyruvate (both from Gibco, Life Technologies) and 60 μg/ml Hygromycin B (AG Scientific Inc). 400 μg/ml Geneticin (Gibco, Life Technologies) was added to maintain stable ovalbumin expression. The 293 cell line was also cultured under the same conditions as B16-F10. For

mRNA isolation and cDNA synthesis, the spleen-derived D1 dendritic cell line was used and cultured as previously described [56].

#### 4.2. Mice

C57BL/6J mice (male and female, 6–8 weeks old) were purchased either from Charles River Laboratories (L’Arbresle, France) or from Janvier Labs (Le Genest Saint Isle, France). B6 Albino mice (strain B6/Rj-Tyr<sup>c/c</sup>) were purchased from Janvier Labs (Le Genest Saint Isle, France). Mice were housed in individually ventilated

cages with enrichment under specific pathogen-free conditions at the LUMC animal facility. All mice experiments were conducted in accordance with Dutch Animal Ethical Committee guidelines. All *in vivo* protocols were approved by the Animal Welfare Body of LUMC.

#### 4.3. Plasmid DNA constructs

The DNA constructs coding for mediators of pyroptosis (**supplementary Table 1**) as well as coding for the antigens (**supplementary Table 2**) were generated by Gibson assembly. DNA sequences of interest were amplified from D1 cells cDNA and cloned into vector pD2610-v10 (ATUM, Newark, CA, USA) using a Gibson Assembly Cloning Kit (New England Biolabs, Ipswich, MA, USA). For vaccination experiments, a polyepitope DNA vaccine coding for five 35-mer antigens separated by a three-alanine (AAA) spacer was used (**supplementary Table 2**). This DNA encoded, from the N- to the C-terminus: three tumor-specific antigens (Dpagt1, Reps1, Adpgk) derived from the C57BL/6 MC38 colon carcinoma cell line [38], as well as a CD4 and a CD8 T cell epitope derived from chicken ovalbumin (ISQAVHAAHAEINEA, SIINFELK). All plasmids were grown using *E. coli* cultures and were purified using a Macherey-Nagel (Dueren, Germany) Endotoxin-Free plasmid purification kit. For vaccination experiments, plasmids underwent an additional purification step on a Macherey-Nagel Nucleobond filter, followed by centrifugation (30 min, 10,000 g, 4 °C) to remove any remaining debris.

#### 4.4. Western blot

293 cells were seeded in 6-well plates, at a density of 600,000 cells in 2 ml of culture medium. The following day, cells were transfected with the DNA constructs complexed with SAINT-DNA (Synvolux products, Leiden, the Netherlands). One day later, wells were either treated with 800  $\mu$ M Z-VAD-FMK (APEX-BIO) or left untreated. Two days after transfection, cells were washed with ice-cold PBS and harvested. After 5 min centrifugation at 1,500 rpm, the supernatant was discarded and the cells were lysed in RIPA buffer supplemented with a protease inhibitor (Sigma Aldrich, location) and a Benzoyl Nuclease (Sigma Aldrich, location) for 30 min under constant agitation at 4 °C. The protein lysates were cleared from the debris by centrifugation at 16,000xg for 20 min at 4 °C. The protein concentrations of the lysates were measured using a BCA Protein assay (Thermo Scientific, location). Equal amounts of total proteins were separated by SDS-PAGE gel and transferred to nitrocellulose membrane. The membranes were blocked in PBS-T with 3% BSA and 0.5% v/v Tween20 overnight at 4 °C followed by 30 min at room temperature (RT) and then incubated for 1 h with the primary antibody  $\alpha$ -p20 (biotin) at RT. After another hour incubation with streptavidin-HRP (Genetex), location and StrepTactin-HRP conjugate (Bio-Rad, location), the signals were detected using enhanced chemiluminescence (Bio-Rad) and the image was captured using ChemiDoc XRS + System (Bio-Rad). The membrane was then stripped using a mild stripping buffer, blocked again and incubated with the primary antibody  $\alpha$ -alpha tubulin (Genetex) for 1 h at RT. After another hour incubation with the secondary antibody HRP Goat anti-rat IgG (BioLegend) and StrepTactin-HRP conjugate, the signals were detected using enhanced chemiluminescence ECL and the image was captured using Chemidoc XRS + System.

#### 4.5. *In vitro* transfections

B16-F10 or 293 cells were plated at 2,000 cells/well or 20,000 cells/well, respectively, in a 96-well flat bottom plate in 100  $\mu$ l culture medium. One day later, cells were transfected by the addition

of DNA complexed with SAINT-DNA (Synvolux products, Leiden, the Netherlands). Two days after transfection, release of IL-1 $\beta$  and/or cell death were analyzed by ELISA, LDH release assay or flow cytometry.

#### 4.6. IL-1 $\beta$ ELISA

B16-F10 cells were transfected with 0.5 ng of the indicated different variants of caspase-1 plasmids and 10 ng pro-IL-1 $\beta$  plasmids, supplemented with empty vector plasmid to 20 ng total plasmid. Two days after transfection, plates were centrifuged, supernatants were harvested and analyzed by ELISA for IL-1 $\beta$  release using protocols provided by the supplier (BioLegend, San Diego, CA). Briefly, 96-well plates were coated with capture antibody overnight. After washing away unbound antibody, 50–5,000-fold diluted supernatant was added and incubated for 2 h at RT while shaking. After washing steps, biotinylated detection antibody was added and incubated for 1 h at RT, followed by another wash steps and a 30 min incubation with streptavidin-HRP. After washing away streptavidin-HRP, TMB substrate solution was added. Absorbance at 450 nm and 570 nm was read on a Tecan Infinite F50 (Tecan Group Ltd, Männedorf, Switzerland). IL-1 $\beta$  concentrations in test samples were determined by interpolation of titrated calibration curves of recombinant mouse IL-1 $\beta$  (BioLegend, San Diego, CA).

#### 4.7. LDH release assay

293 cells were transfected with 10 ng of the indicated different variants of caspase-1 plasmids mixed with 10 ng wild-type gasdermin D DNA (Gsdmd\_WT DNA). Two days after transfection, supernatants were harvested after centrifugation. A colorimetric assay to quantitatively measure lactate dehydrogenase (LDH) released into the culture media (LDH assay kit Promega) was used to quantify cell death.

#### 4.8. Cell death analysis by flow cytometry (7-AAD staining)

B16-F10 cells were transfected with 25 ng GFP-plasmid mixed with 25 ng of the indicated caspase-1 or Gsdmd plasmids, or with a control DNA plasmid encoding an irrelevant 40-mer peptide (Reps1). Two days after transfection, supernatants (including detached cells) were collected, wells were washed with PBS and the remaining adherent cells were treated with trypsin-EDTA. Collected supernatants were then transferred into the corresponding trypsinized wells and transferred to a 96-well V-bottom plate, after which the plate was centrifuged and washed with FACS buffer (PBS, 1% BSA, 0.02% azide). Cells were stained for 15 min with 7-aminoactinomycin D (7-AAD) (BioLegend, San Diego, CA, USA), and immediately acquired on a Guava EasyCyte flow cytometer (Merck Millipore, Burlington, MA, USA).

#### 4.9. Bioluminescence imaging

On day 0, B6 Albino mice were vaccinated intradermally at their tail base either with a control plasmid, a plasmid encoding luciferase (Luc-Ag), or a luciferase plasmid in combination with different doses of active caspase-1 plasmid (Luc-Ag + Casp1). For *in vivo* bioluminescence imaging, on days 1, 6, 9, 13 and 16, mice were injected subcutaneously with 150 mg/kg D-luciferin (Synchem; Cat. Nr. bc219) diluted in DPBS. After 12 min, mice were anaesthetized by isoflurane inhalation and the imaging was performed using IVIS Spectrum small animal imager (PerkinElmer). The luminescent signal was measured using a 540 nm filter and an automatic acquisition time and the photon flux was quantified at the tail base of the mice using fixed-sized regions of interest through-

out the entire experiment. The analysis was performed using LivingImage software (PerkinElmer).

#### 4.10. Vaccination studies

Naïve C57BL/6J mice were primed intradermally and then boosted after 38 days at their tail base with 30 µl endotoxin-free plasmid solutions (in 0.9% NaCl) as mentioned in each figure. Within the same experiment, all mice received the same amount of DNA vaccine combined either with a control plasmid or other DNA constructs. Control mice received a control plasmid, unless mentioned otherwise in the figures legends.

#### 4.11. Flow cytometry

For monitoring antigen-specific T cells, blood was collected via tail puncture in heparinized tubes. Erythrocytes were lysed using erythrocyte lysis buffer (LUMC pharmacy); cells were washed with PBS (LUMC pharmacy) supplemented with 0.1% bovine serum albumin and 0.02% sodium azide (LUMC pharmacy) (PBS/BSA) and stained for 30 min at RT in the dark with a mix of the following antibodies: anti-CD8a BV605 (BioLegend; Cat#: 100744), anti-CD3 BV510 (BD Horizon; Cat#: 563024), APC-conjugated H2-K<sup>b</sup>/SIINFEKL tetramer (LUMC tetramer facility, Leiden, the Netherlands), PE-conjugated H2-D<sup>b</sup>/Adpgk tetramer (LUMC tetramer facility, Leiden, the Netherlands). For compensation staining, the following antibodies were used: anti-CD3 APC (eBioscience; Cat#: 17-0031-83), anti-CD8a BV605 (BioLegend; Cat#: 100744), anti-CD3 BV510 (BD Horizon; Cat#: 563024). 7-AAD (LUMC) was used with the antibody mix as a dead cell marker. Cells were then washed with PBS/BSA and acquired with a BD FACS LSR II 4L Full (BD Biosciences, San Jose, CA, USA) and analyzed using FlowJo software version 10.5.3. Antigen-specific T cell frequencies are expressed as a percentage of gated CD8<sup>+</sup> T cells.

#### 4.12. In vivo specific killing assay

Mice from the vaccination study (Fig. 2d-i) received peptide-loaded splenocytes in order to evaluate the cytotoxic activity of the vaccine generated SIINFEKL-specific T cells. To this end, naïve C57BL/6J mice were sacrificed, their spleens and lymph nodes harvested, manually cut into small pieces and incubated with liberase (Liberase™ TL Research Grade, Roche) for 20 min at 37 °C. The reaction was stopped by adding EDTA and filtering the spleens and lymph nodes through a 70 µm cell strainer. Splenocytes, diluted at 1x10<sup>7</sup> cells/ml, were first differentially loaded with either an irrelevant peptide (5 µg/ml) or SIINFEKL peptide (5 µg/ml) for 2 h at 37 °C. After several PBS/0.1 %FCS wash steps, cells were labelled with either 5 µM (irrelevant peptide loaded cells) or 1 µM (SIINFEKL-loaded cells) CFSE (ThermoFischer) for 10 min at 37 °C. Vaccinated mice then received intravenously a 1:1 ratio mixed 8 million peptide-loaded cells (serving as target cells) in 200 µl PBS. Two days after cell transfer, vaccinated mice were sacrificed, their spleen, processed and evaluated *ex vivo* by flow cytometry for the *in vivo* specific killing. Specific killing was calculated using the following equation:

$$\text{Specific killing} = 100 - \left[ 100 * \frac{\left( \frac{\text{CFSE target peptide}}{\text{CFSE irrelevant peptide}} \text{ immunized mice} \right)}{\left( \frac{\text{CFSE target peptide}}{\text{CFSE irrelevant peptide}} \text{ naïve mice} \right)} \right]$$

#### 4.13. Prophylactic vaccination and B16-OVA tumor challenge

Naïve C57BL/6J mice were first vaccinated intradermally with either 20 µg control plasmid, a mix of 10 µg antigen DNA vaccine and 10 µg control plasmid or a mix of 10 µg antigen DNA and

10 µg active caspase-1 plasmid. On day 28 after vaccination, mice were challenged subcutaneously in their flank with 100,000 B16-OVA cells diluted in 200 µl PBS. Tumor growth was monitored every 3–4 days until day 100 and measured using a caliper. Tumor volume was calculated using the formula: Volume (mm<sup>3</sup>) = length × width<sup>2</sup>/2. Mice carrying tumors exceeding 1,000 mm<sup>3</sup> or with a bleeding ulcer were sacrificed.

#### 4.14. Statistical analysis

Statistical analyses were conducted using GraphPad Prism software (version 8.4.2). The data are represented as the average ± SEM. p values were calculated using two-way ANOVA (followed by Sidak's multiple comparisons test), one-way ANOVA (followed by Tukey's multiple comparisons test), Kruskal-Wallis test (followed by Dunn's multiple comparison tests), or Log-rank (Mantel-Cox) test as indicated in the figures' legends. A p-value less than 0.05 was considered to be statistically significant. \* p < 0.05; \*\* p < 0.01; \*\*\* p < 0.001; \*\*\*\* p < 0.0001; ns: not significant.

#### Funding

This work was supported by Dutch Cancer Society (KWF) consortium grant 11157, the Netherlands Enterprise Agency (Rijksdienst voor Ondernemend Nederland, RVO), Innovation Credit (IK17065).

#### Data availability

The datasets generated during and/or analyzed during the current study are available from the corresponding author on reasonable request.

#### Author Contributions

TA, KO, RA, GZ, FO and JvB designed the experiments. TA, KO, ET, ML, JV, MvG, MC, BT and IZ performed experiments. TA, KO, RA, GZ, FO and JvB interpreted the experiments. TA and JvB wrote the manuscript. All authors contributed to and approved the final manuscript.

#### Declaration of Competing Interest

BT, GZ and JvB are employees of Immunetune. IZ and GZ are employees of Synvolux. JvB and GZ are inventors on patent application WO2020204714A1: 'Immune-stimulatory compositions and use thereof'.

#### Appendix A. Supplementary data

Supplementary data to this article can be found online at <https://doi.org/10.1016/j.vaccine.2022.02.028>.

#### References

- [1] Allen A, Wang C, Caproni IJ, Sugiyarto G, Harden E, Douglas LR, et al. Linear doggybone DNA vaccine induces similar immunological responses to conventional plasmid DNA independently of immune recognition by TLR9 in a pre-clinical model. *Cancer Immunol Immunother* 2018;67(4):627–38.
- [2] Xia Q et al. Anti-tumor effects of DNA vaccine targeting human fibroblast activation protein alpha by producing specific immune responses and altering tumor microenvironment in the 4T1 murine breast cancer model. *Cancer Immunol Immunother* 2016;65(5):613–24.
- [3] Witt K, Ligtenberg MA, Conti L, Lanzardo S, Ruijter R, Wallmann T, et al. Cripto-1 Plasmid DNA Vaccination Targets Metastasis and Cancer Stem Cells in Murine Mammary Carcinoma. *Cancer Immunol Res* 2018;6(11):1417–25.

- [4] Lopes A, Vanvarenberg K, Pr eat V, Vandermeulen G. Codon-Optimized P1A-Encoding DNA Vaccine: Toward a Therapeutic Vaccination against P815 Mastocytoma. *Mol Ther Nucleic Acids* 2017;8:404–15.
- [5] Duperret EK, Perales-Puchalt A, Stoltz R, G.h. H, Mandloi N, Barlow J, et al. A Synthetic DNA, Multi-Neoantigen Vaccine Drives Predominately MHC Class I CD8(+) T-cell Responses, Impacting Tumor Challenge. *Cancer Immunol Res* 2019;7(2):174–82.
- [6] Ottensmeier, C., et al., in Wilms' tumour antigen 1 Immunity via DNA fusion gene vaccination in haematological malignancies by intramuscular injection followed by intramuscular electroporation: a Phase II non-randomised clinical trial (WIN). 2016: Southampton (UK).
- [7] Butterfield LH et al. Alpha fetoprotein DNA prime and adenovirus boost immunization of two hepatocellular cancer patients. *J Transl Med* 2014;12:86.
- [8] Tiriveedhi V, Tucker N, Herndon J, Li L, Sturmoski M, Ellis M, et al. Safety and preliminary evidence of biologic efficacy of a mammaglobin-a DNA vaccine in patients with stable metastatic breast cancer. *Clin Cancer Res* 2014;20(23):5964–75.
- [9] Norell H et al. Vaccination with a plasmid DNA encoding HER-2/neu together with low doses of GM-CSF and IL-2 in patients with metastatic breast carcinoma: a pilot clinical trial. *J Transl Med* 2010;8:53.
- [10] Corr M et al. Costimulation provided by DNA immunization enhances antitumor immunity. *J Immunol* 1997;159(10):4999–5004.
- [11] Kim JJ, Simbiri KA, Sin JJ, Dang K, Oh J, Dentshev T, et al. Cytokine molecular adjuvants modulate immune responses induced by DNA vaccine constructs for HIV-1 and SIV. *J Interferon Cytokine Res* 1999;19(1):77–84.
- [12] van Duin D, Medzhitov R, Shaw AC. Triggering TLR signaling in vaccination. *Trends Immunol* 2006;27(1):49–55.
- [13] Apostolico Jde S et al. Adjuvants: Classification, Modus Operandi, and Licensing. *J Immunol Res* 2016;2016:1459394.
- [14] Song K, Chang Y, Prud'homme GJ. IL-12 plasmid-enhanced DNA vaccination against carcinoembryonic antigen (CEA) studied in immune-gene knockout mice. *Gene Ther* 2000;7(18):1527–35.
- [15] Yang Y, Shao Z, Gao J. Antitumor Effect of a DNA Vaccine Harboring Prostate Cancer-Specific Antigen with IL-12 as an Intramolecular Adjuvant. *J Mol Microbiol Biotechnol* 2017;27(3):168–74.
- [16] Sun Y, Peng S, Yang A, Farmer E, Wu T-C, Hung C-F. Coinjection of IL2 DNA enhances E7-specific antitumor immunity elicited by intravaginal therapeutic HPV DNA vaccination with electroporation. *Gene Ther* 2017;24(7):408–15.
- [17] Yamano T, Kaneda Y, Huang S, Hiramatsu SH, Hoon DSB. Enhancement of immunity by a DNA melanoma vaccine against TRP2 with CCL21 as an adjuvant. *Mol Ther* 2006;13(1):194–202.
- [18] Dorgham K, Abadie V, Iga M, Hartley O, Gorochov G, Combadi ere B. Engineered CCR5 superagonist chemokine as adjuvant in anti-tumor DNA vaccination. *Vaccine* 2008;26(26):3252–60.
- [19] Hornung V, Bauernfeind F, Halle A, Samstad EO, Kono H, Rock KL, et al. Silica crystals and aluminum salts activate the NALP3 inflammasome through phagosomal destabilization. *Nat Immunol* 2008;9(8):847–56.
- [20] Aimanianda V, Haensler J, Lacroix-Desmazes S, Kaveri SV, Bayry J. Novel cellular and molecular mechanisms of induction of immune responses by aluminum adjuvants. *Trends Pharmacol Sci* 2009;30(6):287–95.
- [21] Shi Y, Evans JE, Rock KL. Molecular identification of a danger signal that alerts the immune system to dying cells. *Nature* 2003;425(6957):516–21.
- [22] Vande Walle L, Lamkanfi M. Pyroptosis. *Curr Biol* 2016;26(13):R568–72.
- [23] Bergsbaken T, Fink SL, Cookson BT. Pyroptosis: host cell death and inflammation. *Nat Rev Microbiol* 2009;7(2):99–109.
- [24] Zheng D, Liwinski T, Elinav E. Inflammasome activation and regulation: toward a better understanding of complex mechanisms. *Cell Discov* 2020;6:36.
- [25] Kool M, Soull ie T, van Nimwegen M, Willart MAM, Muskens F, Jung S, et al. Alum adjuvant boosts adaptive immunity by inducing uric acid and activating inflammatory dendritic cells. *J Exp Med* 2008;205(4):869–82.
- [26] Man SM, Karki R, Kanneganti T-D. Molecular mechanisms and functions of pyroptosis, inflammatory caspases and inflammasomes in infectious diseases. *Immunol Rev* 2017;277(1):61–75.
- [27] Iyer SS, Pulsikens WP, Sadler JJ, Butter LM, Teske GJ, Ulland TK, et al. Necrotic cells trigger a sterile inflammatory response through the Nlrp3 inflammasome. *Proc Natl Acad Sci U S A* 2009;106(48):20388–93.
- [28] He WT et al. Gasdermin D is an executor of pyroptosis and required for interleukin-1beta secretion. *Cell Res* 2015;25(12):1285–98.
- [29] Shamaa OR et al. Monocyte Caspase-1 Is Released in a Stable, Active High Molecular Weight Complex Distinct from the Unstable Cell Lysate-Activated Caspase-1. *PLoS One* 2015;10(11):e0142203.
- [30] Miao EA, Rajan JV, Aderem A. Caspase-1-induced pyroptotic cell death. *Immunol Rev* 2011;243(1):206–14.
- [31] Xia S, Hollingsworth LR, Wu H. Mechanism and Regulation of Gasdermin-Mediated Cell Death. *Cold Spring Harb Perspect Biol* 2020;12(3):a036400. <https://doi.org/10.1101/cshperspect.a036400>.
- [32] Yatim N, Cullen S, Albert ML. Dying cells actively regulate adaptive immune responses. *Nat Rev Immunol* 2017;17(4):262–75.
- [33] Srinivasula SM, Ahmad M, MacFarlane M, Luo Z, Huang Z, Fernandes-Alnemri T, et al. Generation of constitutively active recombinant caspases-3 and -6 by rearrangement of their subunits. *J Biol Chem* 1998;273(17):10107–11.
- [34] Park K, Kuechle MK, Choe Y, Craik CS, Lawrence OT, Presland RB. Expression and characterization of constitutively active human caspase-14. *Biochem Biophys Res Commun* 2006;347(4):941–8.
- [35] Broz P, Monack DM. Molecular mechanisms of inflammasome activation during microbial infections. *Immunol Rev* 2011;243(1):174–90.
- [36] Shi J, Zhao Y, Wang K, Shi X, Wang Y, Huang H, et al. Cleavage of GSDMD by inflammatory caspases determines pyroptotic cell death. *Nature* 2015;526(7575):660–5.
- [37] Tondini E, Arakelian T, Oosterhuis K, Camps M, van Duikerens S, Han W, et al. A poly-neoantigen DNA vaccine synergizes with PD-1 blockade to induce T cell-mediated tumor control. *Oncimmunology* 2019;8(11):1652539. <https://doi.org/10.1080/2162402X.2019.1652539>.
- [38] Yadav M, Jhunjhunwala S, Phung QT, Lupardus P, Tanguay J, Bumbaca S, et al. Predicting immunogenic tumour mutations by combining mass spectrometry and exome sequencing. *Nature* 2014;515(7528):572–6.
- [39] Gupta S, Termini JM, Issac B, Guirado E, Stone GW, Liang C. Constitutively Active MAVS Inhibits HIV-1 Replication via Type I Interferon Secretion and Induction of HIV-1 Restriction Factors. *PLoS ONE* 2016;11(2):e0148929. <https://doi.org/10.1371/journal.pone.0148929>.
- [40] Alyaqoub FS, Aldhamen YA, Koestler BJ, Bruger EL, Seregin SS, Pereira-Hicks C, et al. In Vivo Synthesis of Cyclic-di-GMP Using a Recombinant Adenovirus Preferentially Improves Adaptive Immune Responses against Extracellular Antigens. *J Immunol* 2016;196(4):1741–52.
- [41] Tse SW et al. mRNA-encoded, constitutively active STING(V155M) is a potent genetic adjuvant of antigen-specific CD8(+) T cell response. *Mol Ther* 2021;29(7):2227–38.
- [42] Gargett T, Grubor-Bauk B, Garrod TJ, Yu W, Miller D, Major L, et al. Induction of antigen-positive cell death by the expression of perforin, but not DTA, from a DNA vaccine enhances the immune response. *Immunol Cell Biol* 2014;92(4):359–67.
- [43] Grubor-Bauk B, Yu W, Wijesundara D, Gummow J, Garrod T, Brennan AJ, et al. Intradermal delivery of DNA encoding HCV NS3 and perforin elicits robust cell-mediated immunity in mice and pigs. *Gene Ther* 2016;23(1):26–37.
- [44] Albert ML et al. Immature dendritic cells phagocytose apoptotic cells via alphaVbeta5 and CD36, and cross-present antigens to cytotoxic T lymphocytes. *J Exp Med* 1998;188(7):1359–68.
- [45] Kim TW, Hung C-F, Ling M, Juang J, He L, Hardwick JM, et al. Enhancing DNA vaccine potency by coadministration of DNA encoding antiapoptotic proteins. *J Clin Invest* 2003;112(1):109–17.
- [46] T uting T, Storkus WJ, Falot LD. DNA immunization targeting the skin: molecular control of adaptive immunity. *J Invest Dermatol* 1998;111(2):183–8.
- [47] Cao Y, Zhang Q, Xu L, Li S, Wang Di, Zhao J, et al. Effects of different cytokines on immune responses of rainbow trout in a virus DNA vaccination model. *Oncotarget* 2017;8(68):112222–35.
- [48] Cui F-D, Asada H, Jin M-L, Kishida T, Shin-Ya M, Nakaya T, et al. Cytokine genetic adjuvant facilitates prophylactic intravascular DNA vaccine against acute and latent herpes simplex virus infection in mice. *Gene Ther* 2005;12(2):160–8.
- [49] Chow YH et al. Development of Th1 and Th2 populations and the nature of immune responses to hepatitis B virus DNA vaccines can be modulated by codelivery of various cytokine genes. *J Immunol* 1998;160(3):1320–9.
- [50] Dupr e Loic, Kremer L, Wolowczuk I, Riveau G, Capron A, Locht C. Immunostimulatory effect of IL-18-encoding plasmid in DNA vaccination against murine *Schistosoma mansoni* infection. *Vaccine* 2001;19(11-12):1373–80.
- [51] Zhang X, Wang X, Mu L, Ding Z. Immune responses in pigs induced by recombinant DNA vaccine co-expressing swine IL-18 and membrane protein of porcine reproductive and respiratory syndrome virus. *Int J Mol Sci* 2012;13(5):5715–28.
- [52] Staats HF, Ennis Jr FA. IL-1 is an effective adjuvant for mucosal and systemic immune responses when coadministered with protein immunogens. *J Immunol* 1999;162(10):6141–7.
- [53] Van Den Eckhout B et al. Specific targeting of IL-1beta activity to CD8(+) T cells allows for safe use as a vaccine adjuvant. *npj Vaccines* 2020;5:64.
- [54] Deets KA, Vance RE. Inflammasomes and adaptive immune responses. *Nat Immunol* 2021;22(4):412–22.
- [55] Mold M, Shardlow E, Exley C. Insight into the cellular fate and toxicity of aluminium adjuvants used in clinically approved human vaccinations. *Sci Rep* 2016;6:31578.
- [56] Winzler C, Rovere P, Rescigno M, Granucci F, Penna G, Adorini L, et al. Maturation stages of mouse dendritic cells in growth factor-dependent long-term cultures. *J Exp Med* 1997;185(2):317–28.